NASA Contractor Report 145235

(NASA-CR-145235) THREE DIMENSIONAL STEADY AND UNSTEADY ASYMMETRIC FLOW PAST WINGS OF ARBITRARY PLANFORMS (Virginia Polytechnic Inst. and State Univ.) 33 p HC A03/MF A01 CSCL 01A G3/02

N77-33102

Unclas

49406

THREE DIMENSIONAL STEADY AND UNSTEADY ASYMMETRIC FLOW PAST WINGS OF ARBITRARY PLANFORMS

O. A. Kandil, E. H. Atta, and A. H. Nayfeh

NASA Grant NGR 47-004-090

Virginia Polytechnic Institute & State University
Blacksburg, VA 24061

September 1977

National Aeronautics and
Space Administration

Langley Research Center
Hampton, Virginia 23665

THREE DIMENSIONAL STEADY AND UNSTEADY ASYMMETRIC FLOW PAST WINGS OF ARBITRARY PLANFORMS

by

Kandil, O. A.; Atta, E. H.; and Nayfeh, A. H.

Department of Engineering Science and Mechanics
Virginia Polytechnic Institute and State University
Blacksburg, Virginia 24061

SUMMARY

The nonlinear discrete-vortex method has been extended to treat the problem of asymmetric flows past a wing with leading-edge separation, including steady and unsteady flows. The problem is formulated in terms of a body-fixed frame of reference, and the nonlinear discrete-vortex method is modified accordingly. Although the method is general, only examples of flows past delta wings are presented due to the availability of experimental data as well as approximate theories. Comparison of our results with the experimental results of Harvey for a delta wing undergoing a steady rolling motion at zero angle of attack demonstrates the superiority of the present method over existing approximate theories in obtaining highly accurate loads. Numerical results for yawed wings at large angles of attack are also presented. In all cases, total-load coefficients, pressure distributions and shapes of the free-vortex sheets are shown.

LIST OF SYMBOLS

AR	aspect ratio
$b(x)$	local half span
C_ℓ	rolling-moment coefficient
C_p	pressure coefficient
ΔC_p	net pressure coefficient $(C_{p_1} - C_{p_2})$
c_r	root chord
Δc_r	winglet root chord, a characteristic length
$\bar{e}_\infty$	unit vector in the direction of the freestream velocity
$\bar{i},\bar{j},\bar{k}$	unit vectors of wing-fixed frame of reference
ℓ	length of a vortex segment
$\underline{n}$	total number of vortex segments of the model
$\bar{n}_b$	unit normal to the wing surface
$\bar{n}_w$	unit normal to the wake surface
$\bar{r}_j$	position vector of a field point
$S(\bar{r})$	wing surface
$\underline{t}$	dimensionless time
$\bar{U}_\infty$	freestream velocity
$w(\bar{r},t)$	wake surface
x,y,z	wing-fixed frame of reference
$\alpha,\dot{\alpha}$	angle of attack and rate of pitch
$\beta,\dot{\beta}$	angle of yaw and rate of yaw
$\gamma,\dot{\gamma}$	angle of roll and rate of roll
$\bar{\omega}$	angular velocity of wing
Ω	frequency of rolling velocity
ϕ	disturbance velocity potential

Subscripts

i	source point
j	field point
k	time-step number
LE	leading edge
TE	trailing edge
τ	tangent

I. INTRODUCTION

In recent years, development of analytical and numerical methods for predicting the aerodynamic characteristics of wings exhibiting leading-edge and/or wing-tip separation has received considerable attention. The literature contains several analytical methods which are based on simplifying assumptions. These include the assumption that the flow is conical and the assumption that the axial gradients are much smaller than the lateral gradients of the flow properties (slender-body theory). These assumptions represent inaccurate modelling of the full three-dimensional flow and violate the trailing-edge Kutta condition. Methods of this type were presented by Brown and Michael[1], Mangler and Smith[2], and Smith[3].

With the advent of high speed computers, new techniques which avoid these simplifying assumptions were developed. The nonlinear, discrete-vortex technique is among those successful techniques capable of calculating full three-dimensional flows. With this technique, the exact governing equation and the corresponding boundary conditions are satisfied and hence the solution of the inviscid problem is exact in that sense. It is not restricted by the shape of the wing planform or the range of angle of attack as long as vortex breakdown does not occur in the vicinity of the wing (stall phenomenon of wings of low-aspect ratio). However, the separation line is assumed to be known a priori along the sharp edges of the wing. Methods of this type were developed for steady symmetric flows by Belotserkovskii[4], Rehbach[5,6], Kandil[7], Kandil, Mook and Nayfeh[8-11].

Due to the accuracy and simplicity of the nonlinear discrete-vortex technique, it was extended to treat unsteady symmetric flows by Belotserkovskii and Nisht[12], Atta[13], Atta, Kandil, Mook and Nayfeh[14,15]. The source of unsteadiness in the flow may be general, e.g. a sudden translational acceleration of the wing[12], a gust wind which changes the wing angle of attack[13,14], or an oscillatory pitching motion of the wing[15]. The method is characterized by its capability of obtaining the transient as well as the steady-state aerodynamic characteristics of the wing. The technique was also extended by Kandil, Mook, and Nayfeh[16] to treat steady asymmetric flows past a large aspect-ratio rectangular wing. This case is a simulation of the problem of aerodynamic interference which arises when a small aircraft penetrates the wake of a large aircraft. Although the authors didn't account for the wing-tip separation of the trailing wing (due to its large aspect ratio), they did account for the wing-tip separation of the leading wing.

In the present paper, this technique is applied to steady and unsteady asymmetric flows past highly swept-back wings with sharp-edges. Delta wings are chosen as numerical examples due to the availability of experimental and theoretical results. Another reason for this choice is that it represents a severe numerical test of the technique owing to the presence of the vortical spiral cones which emanate from the leading edges and extend over a large portion of the wing surface. Moreover, the free-vortex surfaces are represented by a series of segmented vortex lines which approach the bound-vortex lattice representing the wing surface during the development of the numerical solution. Hence, strong singularities may arise due to the interaction of close vortex lines and therefore safeguards must be imposed to eliminate such singularities.

The problem of steady asymmetric flows was treated earlier by Pullin[17], Hanin and Mishne[18], Jones[19], and Cohen and Nimri[20]. Specifically, the steady flow past a yawed slender delta wing was considered in references 17 and 19 while the flow past a slender delta wing rolling steadily was considered in references 18 and 20. These theories are based primarily on the approximations of slender-body theory. The method of Brown and Michael was extended for the rolling wing[18,20] while the method of Mangler and Smith and the improved method of Smith were extended for the yawed wing[17,19].

Therefore, with these approximations as well as the simplified approximate modelling of the vortex sheets shed from the leading edges, one may expect substantial differences between the predicted and the experimental results. In fact, in all asymmetric results of these theories substantial errors exist in predicting the suction peak of the pressure near the leading edges. This was the case on the receding face of a rolling delta wing at zero angle of attack as reported in references 18 and 20. For the case of a yawed wing at high angle of attack, large errors were reported in predicting the suction peak of the pressure on the windward side of the wing[17,19]. In the latter case the errors were attributed to the substantial secondary separation which develops due to the adverse pressure gradients on the windward side of the wing.

From our point of view, this is only one portion of the cause because as it is well-known the problem of secondary separation is a viscous phenomenon and it cannot be treated by an inviscid model. The other portion of the cause is in fact the modelling of the separated flow and the slender-body assumption . Moreover, on the leeward side of the wing, the core of the primary vortex moves outboard as the angle of yaw is increased. Hence the suction peak on this side disappears and so does the adverse pressure gradients. Thus, secondary separation diminishes and one can expect an inviscid three-dimensional model to yield highly accurate results on the leeward side.

On the experimental side, Fink[21] and Harvey[22] considered steady flows over yawed slender-delta wings. Later, Harvey[23] considered flows over a steadily rolling delta wing. Pressure distributions, local rolling-moment coefficients, local normal-force coefficients, total-load coefficients and positions of the vortex cores were reported in these experiments. These data are used by many investigators for checking the accuracy of their theories. In the present paper, we also consider the same data to check our results for steady asymmetric flows. We also compare our results with available approximate theories. The method is also extended to the problem of unsteady asymmetric flows past a rolling wing.

II. FORMULATION OF THE PROBLEM

We consider a thin delta wing in a uniform stream and let $\overline{U}_\infty$ be the free stream velocity and oxyz be a wing-fixed frame of reference. The wing edges lie in the xy-plane, the x-axis bisects its apex angle and the xz-plane is its plane of symmetry. Euler's angles α, β and γ are used to define the angle of attack, the angle of yaw and the angle of roll of the wing, respectively, see Figure 1. To construct these angles in this order, we start from a position where $\overline{U}_\infty$ is parallel to the x-axis and successively allow for the positive rotations α,β,γ about the y,z, and x axes, respectively. The unit vector $\overline{e}_\infty$ in the direction of the freestream velocity is expressed in terms of these angles and the base unit vectors of the fixed-frame of reference by

$$\overline{e}_\infty = \cos\alpha\,\cos\beta\,\overline{i} + (\sin\alpha\,\sin\gamma - \cos\alpha\,\sin\beta\,\cos\gamma)\overline{j} + (\sin\alpha\,\cos\gamma + \cos\alpha\,\sin\beta\,\sin\gamma)\overline{k} \quad (1)$$

Next, we assume that the wing is rotating with an angular velocity $\overline{\omega}$ which can be expressed in terms of Euler's angles and their rates of change as

$$\overline{\omega} = \omega_x\overline{i} + \omega_y\overline{j} + \omega_z\overline{k}$$
$$= (\dot{\alpha}\,\sin\beta + \dot{\gamma})\overline{i} + (\dot{\alpha}\,\cos\beta\,\cos\gamma + \dot{\beta}\,\sin\gamma)\overline{j} + (-\dot{\alpha}\,\cos\beta\,\sin\gamma + \dot{\beta}\,\cos\gamma)\overline{k} \quad (2)$$

The fluid flow is assumed to be ideal. The assumption that the wing edges are sharp fixes the separation lines along these edges. Vorticity is shed from these edges in the form of free surfaces of tangential discontinuity (free-vortex sheets). Moreover, the flow is assumed to be irrotational in the region R exterior to the wing and its free-vortex sheets. Accordingly, the flow in R is governed by Laplace's equation

$$\nabla^2\phi = 0 \quad (3)$$

where $\phi(\overline{r},t)$ is the disturbance potential. On the boundary ∂R, ϕ satisfies the following boundary conditions. The flow must be tangent to the wing surface; that is,

$$(\overline{e}_\infty + \nabla\phi - \overline{\omega} \times \overline{r}) \cdot \overline{n}_b = 0 \qquad \text{on } S(\overline{r}) = 0 \quad (4)$$

where $\overline{n}_b = \nabla S/|\nabla S|$ is the unit normal to the wing surface S. The pressure is continuous and no flow exists across the free-vortex sheets; these dynamic and kinematic conditions yield

$$\Delta C_p = C_{p_1} - C_{p_2} = (\nabla\phi_1 - \nabla\phi_2) \cdot [2(\overline{\omega} \times \overline{r} - \overline{e}_\infty) - \nabla\phi_1 - \nabla\phi_2] - 2\,\frac{\partial}{\partial t}\,(\phi_1 - \phi_2) = 0$$
$$\text{on } w(\overline{r},t) = 0 \quad (5)$$

$$(\overline{e}_\infty + \nabla\phi - \overline{\omega} \times \overline{r}) \cdot \overline{n}_w - \frac{1}{|\nabla w|}\frac{\partial w}{\partial t} = 0 \qquad \text{on } w(\overline{r},t) = 0 \quad (6)$$

where the subscripts 1 and 2 refer to the upper and lower surfaces of the free-vortex sheets, respectively, and $\overline{n}_w = \nabla w/|\nabla w|$ is the unit normal to the free-vortex sheets. The Kutta condition must be satisfied along the edges of separation, that is the flow leaves smoothly off the edges and the pressure is continuous across these edges. These are expressed by

$$(\overline{e}_\infty + \nabla\phi - \overline{\omega} \times \overline{r}) \cdot \overline{n}_b = 0 \qquad \text{on } S\big|_{TE,LE} = 0 \quad (7)$$

and

$$\Delta C_p = (\nabla\phi_1 - \nabla\phi_2) \cdot [2(\overline{\omega} \times \overline{r} - \overline{e}_\infty) - \nabla\phi_1 - \nabla\phi_2] - 2\,\frac{\partial}{\partial t}(\phi_1 - \phi_2) = 0$$

$$\text{on } S\Big|_{TE,LE} = 0 \tag{8}$$

Far from the wing and its free-vortex sheets, the disturbance velocity vanishes; that is,

$$\nabla\phi \to 0 \tag{9}$$

The complexity of the problem stems from the boundary conditions (5) and (6). These conditions are to be satisfied at the free-vortex sheets $w(\overline{r},t)$ which are unknowns of the problem. In fact, both $w(\overline{r},t)$ and $\phi(\overline{r},t)$ are dependent upon each other and hence a numerical solution is fruitful for this situation. In the next section, we discuss the method of solution of the steady problem and describe its extension to the unsteady problem.

III. METHOD OF SOLUTION

1. Nonlinear Discrete-Vortex Method for the Steady Problem

The method of solution of the steady asymmetric flow is obtained by generalizing the approach of Kandil[7] and Kandil, Mook and Nayfeh[8] for the steady symmetric flow. For the sake of completeness, we outline the basic approach and then describe the generalization to the current problem.

In the basic approach of the lifting problem, a lifting surface may be replaced by a bound-vortex sheet with unknown strength. The velocity potential of this sheet satisfies equation (3) in R and the boundary condition (9). Furthermore, this continuous vortex sheet can be accurately approximated by a lattice of bound-vortex filaments with unknown circulations (bound-vortex lattice) provided it is constructed within certain rules. This point will be undertaken later in detail in the next section.

Along the edges of separation no bound-vortex segments are placed; otherwise the Kutta condition, equation (8), will be partially violated. At these edges, the starting vortex is shed and convected with the local velocity and in a steady flow no more vortices are shed thereafter. According to the theorem of spatial conservation of circulation (Kelvin's theorem), the ends of the bound-vortex lattice lines closest to the edges are connected to vortex lines which extend downstream to infinity where the starting vortex is assumed to be. These vortex lines are called free-vortex lines and represent the free-vortex sheet $w(\overline{r})$. So far, the model satisfies equations (3) and (9) and partially satisfies the Kutta condition.

For steady symmetric flows, equations (4) - (8) immediately yield the corresponding boundary conditions upon setting $\omega = 0$ and dropping the time-dependent terms while equation (1) yields the corresponding free stream velocity upon setting $\beta = \gamma = 0$. With the discrete method, the resulting equations are satisfied at certain points on the known surface $S(\overline{r})$ and the still unknown surface $w(\overline{r})$. This is achieved by successive iterative cycles. In the first step of the cycle, we satisfy the flow tangency condition on $S(\overline{r})$ with an assumed surface $w(\overline{r})$ to find a circulation distribution Γ. In the next step, we satisfy the kinematic and dynamic boundary conditions on $w(\overline{r})$ by using the Γ distribution and find $w(\overline{r})$. These cycles are repeated until the Γ distribution or $w(\overline{r})$ do not change within certain prescribed tolerances. The Kutta condition is then satisfied automatically.

For steady asymmetric flows, equations (4) - (8) also yield the corresponding boundary conditions upon dropping the time dependent terms. Now, to obtain a steady flow it is a necessary condition, although not sufficient, that the angular velocity of the wing ω be uniform. Moreover, the magnitude and direction of ω as well as the orientation of the wing with respect to $\overline{e}_\infty$ (as defined by α,β,γ) must have values such that no time-dependent disturbance is generated in the flow. For a thin flat wing with $\overline{\omega} = 0$ ($\dot{\alpha} = \dot{\beta} = \dot{\gamma} = 0$), nontrivial, steady, asymmetric flows occur in three cases. First, $\gamma = 0$ and the free stream velocity is given by

$$\overline{e}_\infty = \cos\alpha \cos\beta \,\overline{i} - \cos\alpha \sin\beta \,\overline{j} + \sin\alpha \,\overline{k} \tag{10a}$$

This case represents the steady flow past a yawed wing at an angle of attack. It was considered in references 17, 19, and 22. Second, $\beta = 0$ and the free stream velocity is given by

$$\overline{e}_\infty = \cos\alpha \,\overline{i} + \sin\alpha \sin\gamma \,\overline{j} + \sin\alpha \cos\gamma \,\overline{k} \tag{10b}$$

This case represents a steady flow past a wing at a banking angle and an angle of attack. Third, $\alpha = 0$ and the free stream velocity is given by

$$\overline{e}_\infty = \cos\beta\ \overline{i} - \sin\beta\ \cos\gamma\ \overline{j} + \sin\beta\ \sin\gamma\ \overline{k} \tag{10c}$$

This case represents a steady flow past a yawed wing at a banking angle. Fourth, when all the angles α, β, and γ are different from zero and the free stream velocity is given by equation (1). All the cases considered above can be treated by the vortex lattice method as reported in references 7-10.

When the angular velocity $\overline{\omega}$ is not equal to zero, there are still two cases where the flow is steady. First, $\alpha = \beta = \dot{\alpha} = \dot{\beta} = 0$, $\overline{\omega} = \dot{\gamma}\overline{i}$ and the free stream velocity is given by

$$\overline{e}_\infty = \overline{i} \tag{11a}$$

This case represents a steadily rolling wing about its x-axis at a zero angle of attack. It was considered in references 18, 20, and 23. Second, $\beta = \gamma = \dot{\alpha} = 0$, $\omega = \dot{\gamma}\overline{i} + \dot{\beta}\overline{k}$, $\tan\alpha = \dot{\beta}/\dot{\gamma}$ and the free stream velocity is given by

$$\overline{e}_\infty = \cos\alpha\ \overline{i} + \sin\alpha\ \overline{k} \tag{11b}$$

This case represents a steadily rolling wing about the wind axis at an angle of attack. We can easily see that the first case is a special case of the present one. This case was considered in reference 20.

When applying the steady version of the discrete-vortex method to the last two cases, one must use a wing-fixed frame of reference; otherwise, the flow would no longer be steady.

2. Nonlinear Discrete-Vortex Method for the Unsteady-Flow Problem

The method of solution for unsteady asymmetric flows is obtained by generalizing the approach of Atta[13] and Atta, Kandil, Mook and Nayfeh[14,15] for unsteady symmetric flows. In these references, a space-fixed frame of reference was used, the wing was taken to be fixed in the flow, and the source of unsteadiness was introduced through the free stream velocity. In the present paper, a wing-fixed frame of reference is used, the wing is rotating at a nonuniform angular velocity $\overline{\omega}(t)$, and the free stream velocity is uniform.

In either case, the bound circulation around the wing continuously changes and this is accompanied by a continuous process of formation and shedding of vortexes from the edges of separation to restore the smoothness of the flow at the edges (Kutta condition). Within any infinitesimal time step, the change in the bound circulation around the wing is met by the formation of an infinitesimal vortex strip emanating from an edge of separation which has a strength of equal and opposite sense to the change of the bound circulation. This shed vortex is convected downstream with the local particle velocity. Hence a vortex sheet is continuously growing downstream as long as the unsteadiness of the flow prevails.

Now if the continuous motion of the wing is discretized into a series of impulsive changes occuring at discrete time steps, the continuously growing vortex sheet can be replaced by a growing vortex lattice in the wake. This is the salient difference between the unsteady and steady flow models. At each time step, we solve the problem using a method similar to that of the steady flow. Here, the boundary conditions, equations (4) - (8), must be satisfied at each time step. In the next section, we consider in detail the implementation of this method.

IV. IMPLEMENTATION OF THE METHOD

1. Construction of the Discrete-Vortex Model

In Figure 2, we show how the discrete-vortex model is constructed for a delta wing. Although the example discussed here is for a thin, flat, delta wing, the method is general and is not restricted by the geometrical parameters of the wing; e.g. camber, aspect or thickness ratios or wing planform.

The first step is to divide the wing into rectangular and cropped-delta winglets as shown by the dashed lines in Figure 2.a. A rectangular winglet is aerodynamically represented by a spanwise bound-vortex segment of constant circulation Γ_i. This segment is placed at the quarter-chord length of the winglet (the chord length of the rectangular winglet is the characteristic length of the problem). In addition a control point is placed at the three quarter-chord length. The choice of these positions is suggested by thin airfoil theory[24]. It can be shown that the bound-vortex sheet representing the two-dimensional flow around a flat plate at an angle of attack can be replaced by a point vortex of the same strength as that of the continuous vortex sheet under the following conditions: a) the point vortex is placed at the quarter-chord length and b) the flow tangency condition is enforced at only one point at the three-quarter-chord length.

On the other hand, a cropped-delta winglet is aerodynamically represented by a bound-vortex segment of constant circulation. This vortex segment is directed along the perpendicular from the midpoint of the winglet root chord to its leading edge. With this choice it can be seen that the vorticity of this vortex segment does not have a component along the leading edge and hence the Kutta condition is approximately satisfied along this edge.

Chordwise bound-vortex segments arise due to the differences in the strengths of the neighboring spanwise, bound-vortex segments. In this way, a bound-vortex lattice which replaces the continuous, bound-vortex sheet is constructed. The model is completed by adding free-vortex lines, representing the continuous free-vortex sheets at the ends of the bound-vortex lattice along the edges of separation - the leading and trailing edges. Each line is divided into a series of small, straight segments (near-wake region) and one semi-infinite vortex line (far-wake region). The upstream end of each segment represents a control point of the wake surface where the kinematic and dynamic boundary conditions are satisfied. The initial positions and shapes of these lines are prescribed. The resulting model is shown in Figure 2b. This model has an unknown circulation distribution and a wake that can be deformed to satisfy the boundary conditions.

The model described above is used to solve the steady-flow problem by satisfying the corresponding boundary conditions given in Section III.1. On the other hand, if the problem under consideration is for an unsteady flow which starts from a steady flow situation, then the solution of the steady-flow problem serves as an initial condition to the unsteady problem. Furthermore, if the problem under consideration is for an unsteady flow which arises from an impulsive motion of the wing, then the initial condition corresponds also to the solution of the model given above, but with the wakes removed from the model.

2. Calculation of the Velocity Field

To satisfy the boundary conditions on the wing and its wake and to calculate the surface pressure distribution, one needs an accurate method to calculate the velocity at any field point $\bar{r}_j$ at any time step t_k. If the field point is off the wing and its wake, then the velocity is given by

$$\overline{V}(\overline{r}_j,t_k) = \nabla\phi(\overline{r}_j,t_k) + \overline{e}_\infty - \overline{\omega}(t_k) \times \overline{r}_j \qquad (12)$$

where

$$\nabla\phi(\overline{r}_j,t_k) = \sum_i^{n(t_k)} [\Gamma_i(t_k)/4\pi h_i(\overline{r}_j,t_k)][\cos\theta_{1i}(\overline{r}_j,t_k) - \cos\theta_{2i}(\overline{r}_j,t_k)]\overline{e}_i(\overline{r}_j,t_k) \qquad (13)$$

is the induced velocity from all the vortex segments of the model. The parameters on the right-hand side of equation (13) are those of Biot-Savart's law[24]. The number of vortex segments $n(t_k)$ is a function of the time step t_k due to the growing vortex lattice in the wake in the unsteady-flow problem. To avoid extremely large induced velocities, an "artificial viscosity" is introduced (as in ref. 25) in the form of an exponential multiplier which causes the induced velocity to approach zero as the vortex is approached.

When the field point is on the wing surface or on the wake surface, one has to account for the induced tangential velocity due to the local strength of the vortex sheet. In Figure 2.c, we show the parameters involved in calculating the components of the induced tangential velocity in the x and y directions at a point p for a quadrilateral vortex element in the xy-plane. With linear interpolation, it is easy to show that these components are given by

$$\overline{V}_{\tau x}(z = {}^{0^+}_{0^-}) = \pm\ (1/2\ \ell_1^2)[\Gamma_1(x_1 + \ell_1 - x) + \Gamma_3(x - x_1)]\overline{e}_1 \qquad (14a)$$

$$\overline{V}_{\tau y}(z = {}^{0^+}_{0^-}) = \mp\ (1/2\ \ell_2^2)[\Gamma_4(y_1 + \ell_2 - y) + \Gamma_2(y - y_1)]\overline{e}_2 \qquad (14b)$$

where the arguments $z = 0^+$ and $z = 0^-$ correspond to the upper surface and the lower surface of the wing, respectively. Equations (14) must be added to equation (12) if one is to calculate the pressure distribution on the upper and lower surfaces by using Bernoulli's equation. Extension of equations (14) to a general, quadrilateral vortex element is straightforward.

3. Implementation of the Boundary Conditions

a. Steady-Flow Problem

The boundary conditions on the wing surface $S(\overline{r})$ and the wake surface $w(\overline{r})$ are satisfied by an iterative process. To initiate the iterative process, one needs to prescribe an initial geometry of the wake surface. It has been found from several numerical tests that the number of iterative cycles required to achieve the solution can be reduced by an appropriate choice of the initial geometry. This initial geometry depends on the problem under consideration and thus it varies from one problem to the other.

For instance, the number of iterative cycles for the steady, symmetric-flow problem is reduced by about 20% when the free-vortex lines emanating from the leading edge are prescribed to be straight lines pitched at one half the wing angle of attack. In addition, those lines emanating from the trailing edge are straight lines pitched at one third the wing angle of attack. Here, the comparison is made with respect to the number of iterative cycles required for the same problem when all the free-vortex lines are prescribed to be also straight lines but are pitched at an angle equal to the wing angle of attack.

In the case of a steadily, rolling wing at zero angle of attack, an appropriate initial guess is found to be related to an angle $\theta(\overline{r}) = \pm \frac{1}{2} \tan^{-1}|\overline{\omega}\times\overline{r}|/U_\infty$. Here, we specify the free-vortex lines emanating from the edges of the advancing side to be straight lines pitched at the angle $+ \theta$ while those emanating from the edges of the receding side to be straight lines pitched at the angle $- \theta$.

Next, the flow-tangency condition and the spatial conservation of circulation are applied at the control points and node points, respectively, of the bound-vortex lattice. Thus, we obtain a set of linear algebric equations[11] which yields the circulation distribution Γ_i.

With the circulation distribution known, the kinematic and dynamic boundary conditions at the control points of the free-vortex lines are satisfied. For steady flows, these two conditions are combined into a simple condition in which we require that each vortex segment in the wake be aligned with the local velocity at its upstream end (a control point on the wake surface). This means that each vortex segment is a segment of a streamline (kinematic condition). Moreover, it means that the force on each vortex segment is zero according to Kutta-Joukowski theorem in the small (dynamic condition). This process is carried out by calculating the downstream end of each vortex segment according to

$$\bar{r}_{j+1} = \bar{r}_j + \bar{V}_j \ell_j / |\bar{V}_j| \tag{15}$$

where $\bar{r}_j$ and $\bar{r}_{j+1}$ are the position vectors of the upstream and downstream ends, respectively, ℓ_j is the segment length and $\bar{V}_k$ is the velocity at its upstream point [equation (12) for steady flows].

The iteration scheme moves back and forth from the control points of the bound-vortex lattice to the control points of the free-vortex lines until convergence is achieved. We consider the iteration scheme converged when the variation in the circulation distribution or the displacement of the downstream ends of the free-vortex segment between two successive iteration cycles does not exceed a certain prescribed tolerance. Once convergence is achieved, we calculate the pressure distribution and the total load coefficients.

b. Unsteady-Flow Problem

Here, we consider the problem of unsteady flow which starts from a steady flow situation. We recall from Section III.2 that the continuous motion of the wing is discretized into a series of impulsive changes occuring at discrete time steps. At each time step t_k, a set of starting vortices develops along the edges of separation and are shed with the local velocities to restore the smoothness of flow at the edges (Kutta condition). In the same time, the starting vortices shed in the wake at earlier time steps are convected downstream with the local velocities without changing their strengths. This process satisfies the kinematic condition on the wake (a wake element moves along the direction of the local velocity) and it also satisfies the dynamic condition on the wake (a wake element satisfies Kelvin-Helmholtz theorem).

The position of any shed vortex $\bar{r}_j$ at any time step t_k is determined by

$$\bar{r}_j(t_k) = \bar{r}_j(t_{k-1}) + (t_k - t_{k-1})\bar{V}_j(\bar{r}_j, t_{k-1}) \tag{16}$$

where t_{k-1} is the preceding time step and $\bar{V}_j$ is given by equation (12). The strength of any newly shed vortex is related to the change in the bound circulation. Hence, with the positions of the shed vortices known from equation (16) and with the strength of the newly shed vortices given in terms of the change of the bound circulation, the flow tangency condition at the control points of the wing yields the unknown circulation distribution. To account for the error in equation (16) because of using the velocity $\bar{V}_j(\bar{r}_j,t_{k-1})$ at the preceding time step t_{k-1} rather than the current time step t_k, an iteration procedure similar to that of the steady-flow problem is performed. In this regard, an alternative equation was given by Summa[26].

In both the steady and unsteady flows, the only difference between the symmetric and asymmetric problems is the longer computational time required for the latter problem as compared to that of the former problem. In the former problem we need only to use half the wing to obtain the solution because of the symmetry of the flow. In the latter problem, the whole wing must be used to obtain the solution.

4. Calculation of the Pressure Coefficients

The distribution of the pressure coefficient on the upper and lower surfaces of the wing is calculated by using Bernoulli's equation in terms of a wing-fixed frame of reference[27].

$$C_p(\bar{r}_j^{\pm},t_k) = -[\bar{v}(\bar{r}_j^{\pm},t_k)]^2 + 2\bar{v}(\bar{r}_j^{\pm},t_k)\cdot[\bar{\omega}(t_k)\times\bar{r}_j - \bar{e}_\infty] - 2\frac{\partial\phi(\bar{r}_j,t_k)}{\partial t} \qquad (17)$$

where

$$\bar{v}(\bar{r}_j^{\pm},t_k) = \nabla\phi(\bar{r}_j,t_k) + \bar{V}_{\tau x}(\bar{r}_j^{\pm},t_k) + \bar{V}_{\tau y}(\bar{r}_j^{\pm},t_k) \qquad (18)$$

$\bar{r}_j^{\pm}$ is the position vector of the control point, the positive and negative superscripts refer to the upper surface and lower surface of the wing, respectively, and $\nabla\phi$, $\bar{V}_{\tau x}$ and $\bar{V}_{\tau y}$ are given by equations (13), (14a) and (14b), respectively. The pressure is calculated at the control points of the bound-vortex lattice because these are the points where the flow tangency condition is enforced.

In the steady-flow problem, the last term of the right-hand side of equation (17) is zero and all the other terms are time independent. Hence, calculating the pressure on the upper and lower surfaces is straightforward. But in the unsteady-flow problem, we need to calculate this term if the pressure coefficient is required on each of the upper and lower surfaces. To calculate the local rate of change of the disturbance velocity potential, we need to know the velocity potential at this location at two successive time steps by integrating the velocity from an undisturbed position. Because of the long computational time involved, we only calculate the net pressure force on the wing in the unsteady-flow problem. However, calculations of the pressure distribution on the upper and lower surfaces are now under consideration because it is necessary for any boundary-layer calculations.

The net pressure coefficient is given by

$$\Delta C_p(\bar{r}_j,t_k) = 4[\bar{V}_{\zeta x}(\bar{r}_j^{+},t_k) + \bar{V}_{\zeta y}(\bar{r}_j^{+},t_k)]\cdot[\bar{\omega}(t_k)\times\bar{r}_j - \bar{e}_\infty - \nabla\phi(\bar{r}_j,t_k)]$$
$$- 2[\Gamma(\bar{r}_j,t_k) - \Gamma(\bar{r}_j,t_{k-1})/(t_k - t_{k-1})] \qquad (19)$$

The total-load coefficients are obtained by integrating the net pressure coefficient on the wing.

V. NUMERICAL RESULTS

A computer code which accounts for the general formulation presented here is developed. The code can be used to solve steady, unsteady, symmetric or asymmetric flow problems. Typical results obtained with this code are presented in this section. The required computation time and convergence studies are discussed in references 7-11 and 13-16.

1. Steadily Rolling Wing at Zero Angle of Attack

In Figures 3-5 we show typical solutions of the free-vortex lines of a delta wing (AR = 0.7) at different rolling velocities 0.2, 0.4 and 0.6. In each figure, a three-dimensional view and a plan view are given. The traces of the helical vortex cones are indicated on the upper view which show that the cones are antisymmetric. The size of the cone increases and it rolls-up more rapidly with increasing the rolling velocity. This is in agreement with the experimental results[23].

Figure 6 shows the spanwise pressure distribution on the upper and lower surfaces at the chordwise station $x/c_r = 0.778$, the present results are compared with the experimental results of Harvey[23] and the theoretical models of references 18 and 20. A remarkable agreement can be seen between the present results and the experimental ones. The methods of references 18 and 20 obviously overestimate the suction pressure peak and this is attributed to the simplified representation of the separated flow.

2. Yawed Wing at an Angle of Attack

In Figures 7-12 we show the effect of the yaw angle on the free-vortex lines and pressure distributions of a delta wing (AR = 0.7, $\alpha = 15°$).

The plan views in Figures 7, 9 and 11 show that the size of vortex cone emanating from the windward side of the wing increases while the size of the cone from the leeward side decreases. The former cone moves inboard while the latter cone moves outboard.

The corresponding effect on the spanwise pressure distribution at the chordwise station $x/c_r = 0.395$ and comparisons with the results of Pullin[17] and the experimental results of Harvey[22] are given in Figures 8, 10 and 12. When the angle of yaw increases, the suction pressure peak on the windward side increases while that on the leeward side decreases. The present results are in a good agreement with the experimental ones. Pullin's results overestimates the suction peak on the windward side of the wing and it shows that the error increases with increasing the angle of yaw.

3. Unsteadily Rolling Wing at Zero Angle of Attack

In Figure 13 we show the free-vortex lines at three successive time steps for a delta wing undergoing an unsteady rolling motion given by $\omega_x = 0.6 + 0.1 \sin(\pi t/6)$. The starting vortices shed from the edges of separation and later convected downstream can be seen in each view.

Figure 14 shows the spanwise pressure distribution at the chordwise state $x/c_r = 0.65$ at different time steps. The variation of the rolling-moment coefficient C_x with the frequency of the sinusoidal variation of the rolling velocity Ω is given in Figure 15. In the initial time steps, we notice that the rolling-moment coefficient decreases as the frequency increases. Finally, the variation of the rolling-moment coefficient with the rate of roll is shown in Figure 16.

VI. CONCLUDING REMARKS

We have presented a general, nonlinear, discrete-vortex method for the lifting surfaces. The method is applied to delta wings undergoing different motions. The results are compared with several results of other investigators and with the experimental results of Harvey. They show that the present method provides accurate results which could not be obtained by the existing approximate methods. Moreover, the present method is not restricted by any geometrical parameter of the lifting surface. Moreover, it is exact because it is free from any small-disturbance assumption or any corresponding linearization.

REFERENCES

1. Brown, C. E. and Michael, W. H., "On Slender Delta Wings with Leading-Edge Separation," NACA Tech. Note 3430, April 1955.
2. Mangler, K. W. and Smith, J. H. B., "A Theory of the Flow Past a Slender Delta Wing with Leading-Edge Separation," Proc. Roy. Soc. Lond. A, 251, 1959, pp. 200-217
3. Smith, J. H. B., "Improved Calculations of Leading-Edge Separation from Slender Delta Wings," Proc. Roy. Soc. Lond. A, 306, 1968, pp. 67-90.
4. Belotserkovskii, S. M., "Calculation of the Flow Around Wings of Arbitrary Planform over a Wide Range of Angle of Attack," NASA TT F-12, 391, May 1969.
5. Rehbach, C., "Calculation of Flow Around Zero-Thickness Wings with Evolute Vortex Sheets," NASA TT F-15, 183, 1973.
6. Rehbach, C., "Numerical Investigation of Vortex Sheets Issuing from Separation Line Near the Leading Edge," NASA TT F-15, 530, 1974.
7. Kandil, O. A., "Prediction of the Steady Aerodynamic Loads on Lifting Surfaces Having Sharp-Edge Separation," Ph.D. Dissertation, Dept. of Engr. Sci. and Mechanics, Virginia Polytechnic Institute and State University, Dec. 1974.
8. Kandil, O. A., Mook, D. T. and Nayfeh, A. H., "Nonlinear Prediction of the Aerodynamic Loads on Lifting Surfaces," J. of Aircraft, Vol. 13, No. 1, January 1976, pp. 27-28.
9. Kandil, O. A., Mook, D. T. and Nayfeh, A. H., "Subsonic Loads on Wings Having Sharp Leading Edges and Tips," J. of Aircraft, Vol. 13, No. 1, January 1976, pp. 62-63.
10. Kandil, O. A., Mook, D. T. and Nayfeh, A. H., "New Convergence Criteria for the Vortex-Lattice Models of the Leading-Edge Separation," NASA SP-405, No. 16, May 1976, pp. 285-300.
11. Kandil, O. A., Mook, D. T. and Nayfeh, A. H., "A Numerical Technique for Computing Subsonic Flow Past Three Dimensional Canard-Wing Configurations with Edge Separation," AIAA Paper No. 77-1, January 1977.
12. Belotserkovskii, S. M. and Nisht, M. I., "Nonstationary Nonlinear Theory of a Thin Wing of Arbitrary Planform," Fluid Dyn. 9(4), 1974, pp. 583-589.
13. Atta, E. H., "Unsteady Flow Over Arbitrary Wing-Planforms Including Tip Separation," M.S. Thesis, Dept. of Engineering Science and Mechanics, Virginia Polytechnic Institute and State University, March 1976.
14. Atta, E. H., Kandil, O. A., Mook, D. T. and Nayfeh, A. H., "Unsteady Flow Past Wings Having Sharp-Edge Separation," NASA SP-405, No. 22, May 1976, pp. 407-418.
15. Atta, E. H. Kandil, O. A., Mook, D. T. and Nayfeh, A. H., Unsteady Aerodynamic Loads on Arbitrary Wings Including Wing-Tip and Leading-Edge Separation," AIAA Paper No. 77-156, January 1977.
16. Kandil, O. A., Mook, D. T. and Nayfeh, A. H., "Application of the Nonlinear Vortex-Lattice Concept to Aircraft-Interference Problems," Advances in Engineering Science, Vol. 4, NASA CP-2001, Nov. 1976, pp. 1321-1330.
17. Pullin, D. I., "Calculations of the Steady Conical Flow Past a Yawed Slender Delta Wing with Leading Edge Separation," Imperial College of Science and Technology, Lond., I.C. Aero Report 72-17, July 1972.
18. Hanin, M. and Mishne, D., "Flow About a Rolling Slender Wing with Leading Edge Separation," Israel Journal of Technology, Vol. 11, No. 3, 1973, pp. 131-136.
19. Jones, I. P., "Flow Separation From Yawed Delta Wings," Computers and Fluids, Vol. 3, 1975, pp. 155-177.
20 Cohen, M. J. and Nimri, D., "Aerodynamics of Slender Rolling Wings at Incidence in Separated Flow," AIAA Journal, Vol. 14, No. 7, July 1976, pp. 886-893.
21. Fink, P. T., "Some Early Experiments on Vortex Separations," British R & M No. 3489, 1967.
22. Harvey, J. K., "Some Measurements on a Yawed Slender Delta Wing with Leading Edge Separation," British ARC Report 20451, 1958.

23. Harvey, J. K., "A Study of the Flow Field Associated with Steadily-Rolling Slender Delta Wing," Journal of the Royal Aeronautical Society, Vol. 68, Feb. 1964, pp. 106-110.
24. Karamcheti, K. PRINCIPLES OF IDEAL-FLUID AERODYNAMICS. John Wiley and Sons, Inc., N.Y. 1966.
25. Yager, P. M., Holland, C. H., and Strand, T., "Modified Weissinger Lifting Surface Method for Calculating Aerodynamic Parameters of Arbitrary Wing-Canard Configurations," Air Vehicle Corporation, La Jolla, Calif., Rept. 354, August 1974.
26. Summa, J. M., "Potential Flow About Three-Dimensional Lifting Configurations with Application to Wings and Rotors," AIAA Paper No. 75-126, 1975.
27. Kochin, N. E., Kibel, I. A., Roze, N.V. THEORETICAL HYDRODYNAMICS, Interscience-Wiley, New York, 1964.

ACKNOWLEDGEMENT

This work was supported by the NASA Langley Research Center under Grant NGR 47-004-090, Dr. E. C. Yates, Monitor.

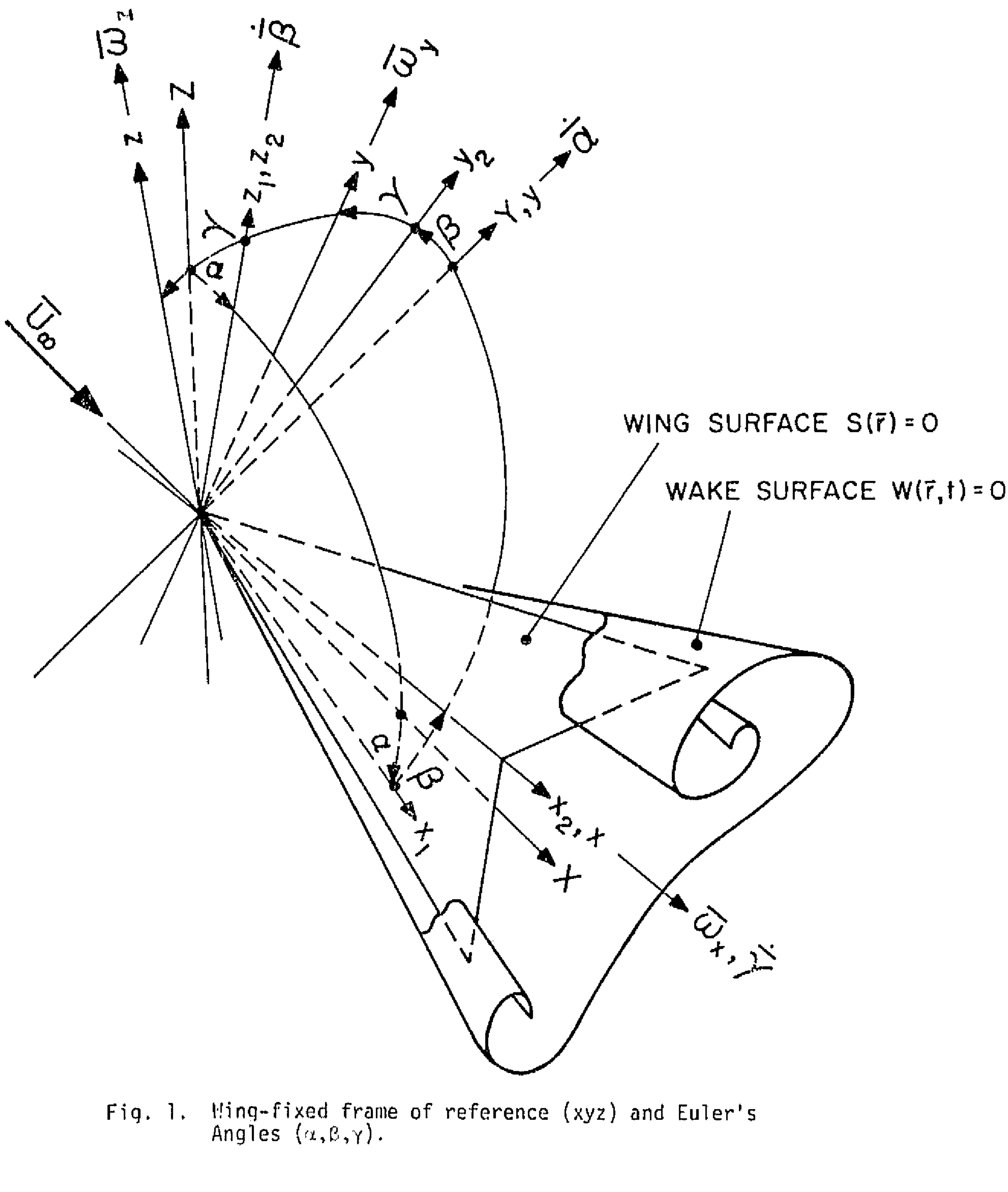

Fig. 1. Wing-fixed frame of reference (xyz) and Euler's Angles (α,β,γ).

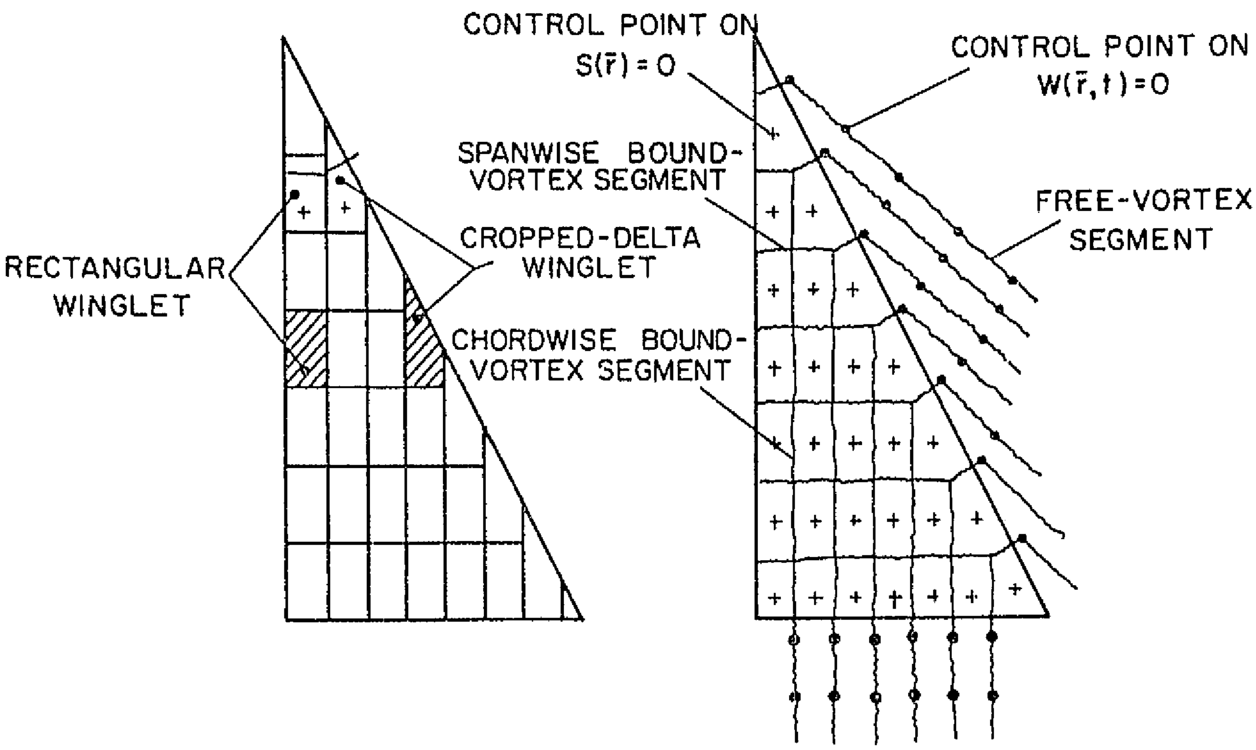

a. Discretization of wing into winglets

b. Discrete-vortex system

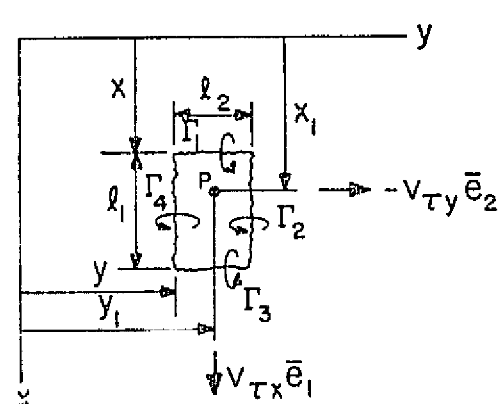

c. Induced tangential velocities

Fig. 2. Construction of the discrete-vortex system.

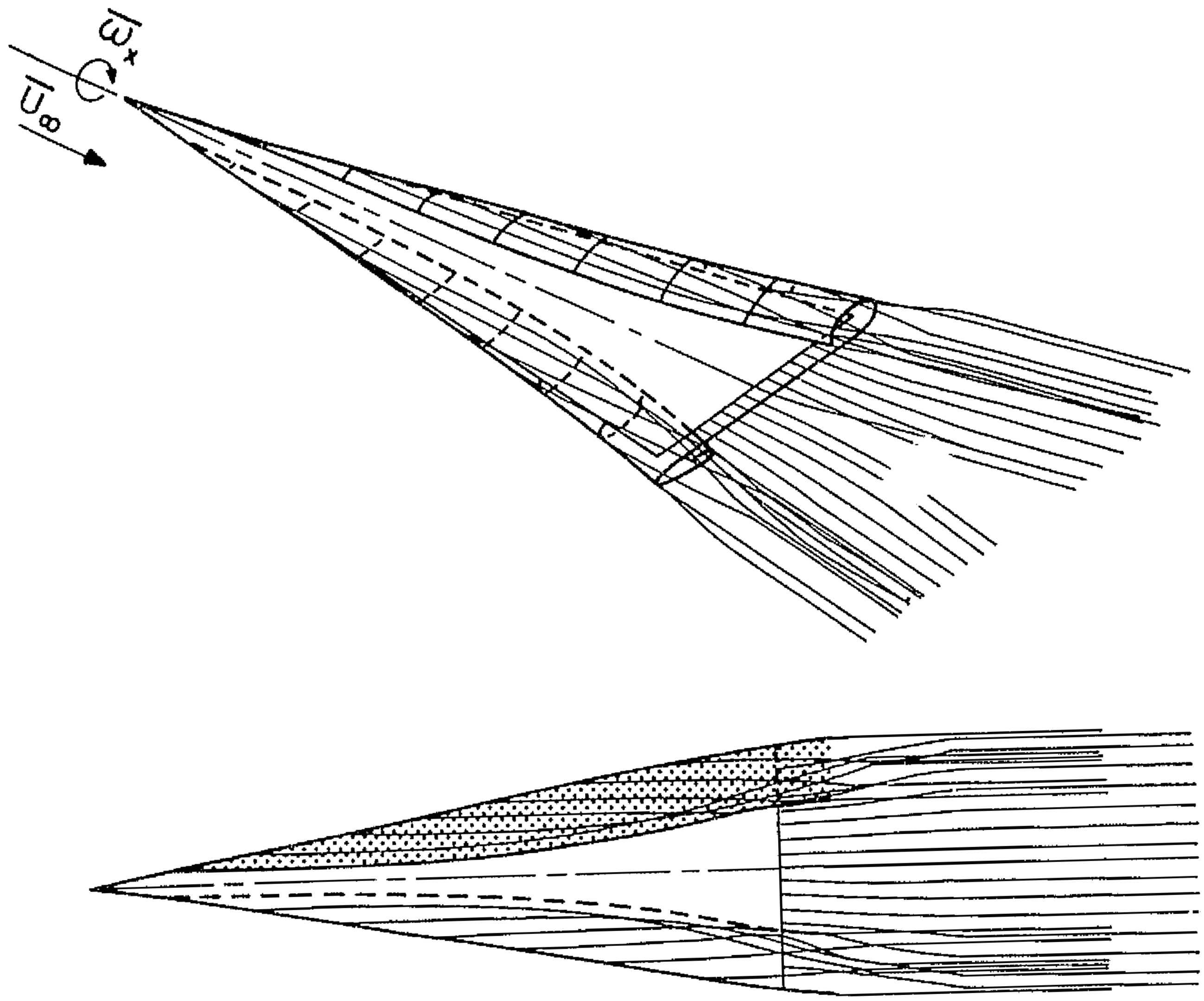

Fig. 3. Wake shape of a steadily rolling delta wing,
$\omega_x = -0.2$, $\alpha = 0°$, 8 x 8 bound lattice, $AR = 0.7$.

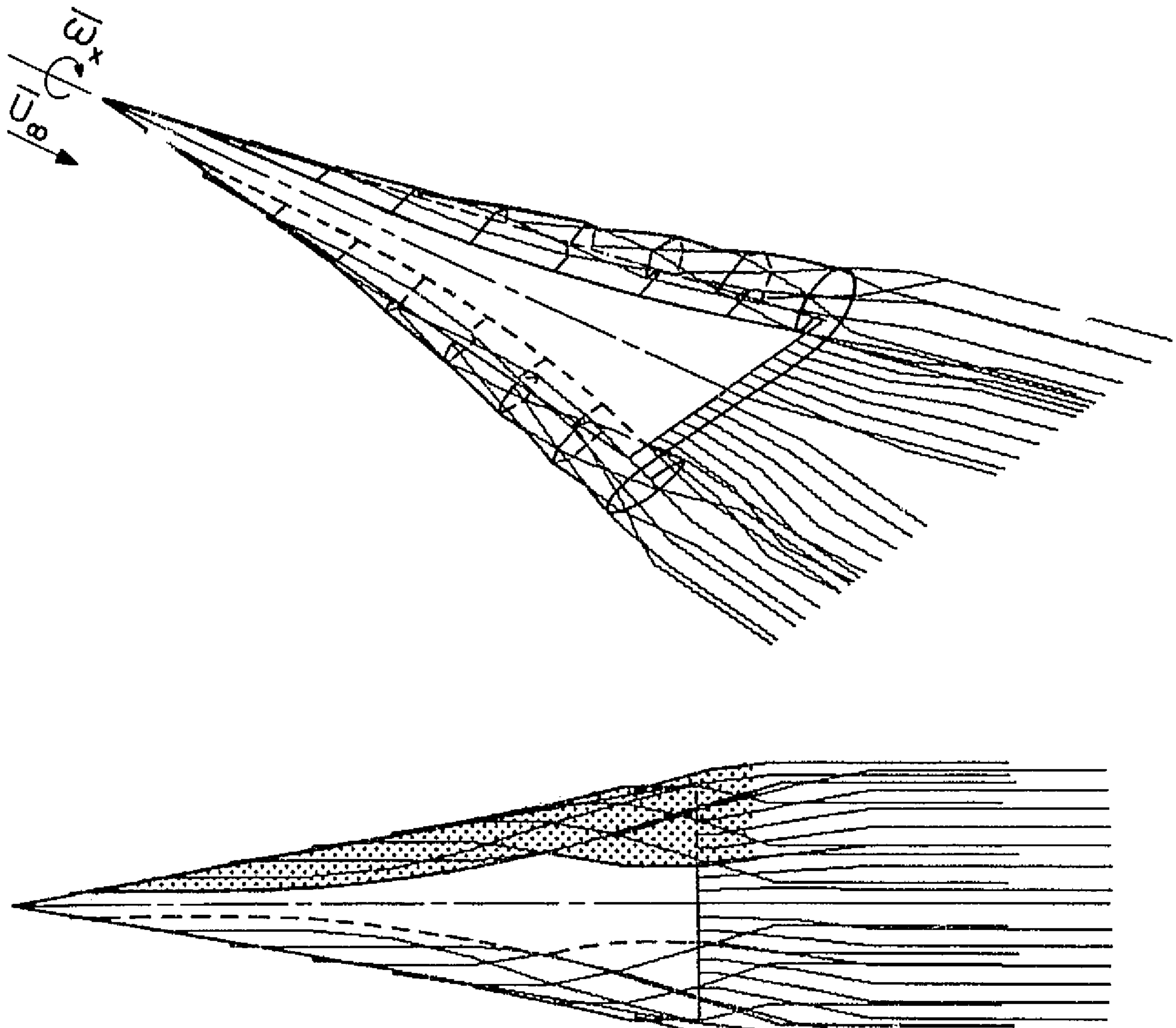

Fig. 4. Wake shape of a steadily rolling delta wing, $\omega_x = -0.4$, $\alpha = 0°$, 8 x 8 bound lattice, AR = 0.7.

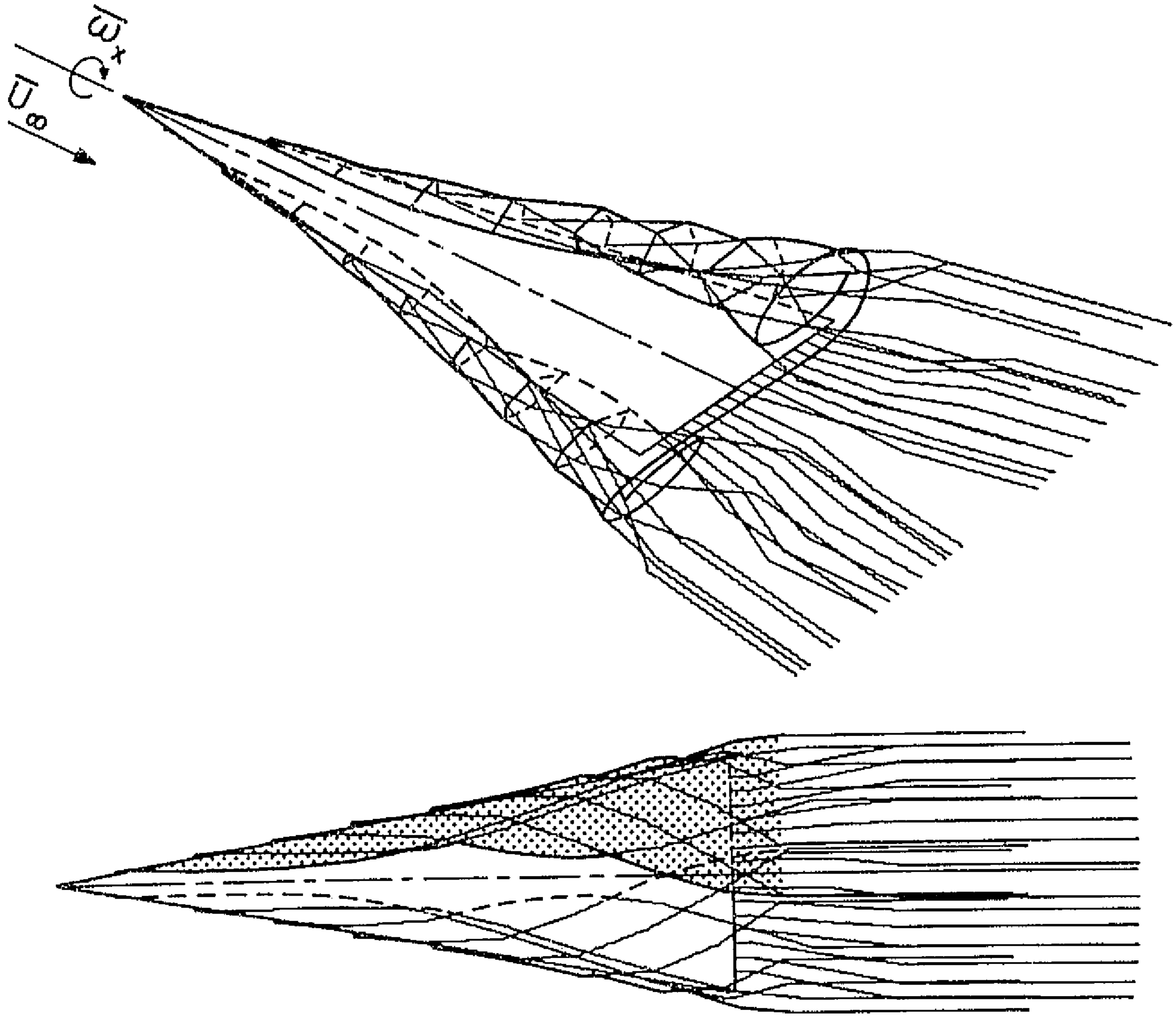

Fig. 5. Wake shape of a steadily rolling delta wing, $\omega_x = -0.6$, $\alpha = 0$, 8 x 8 bound lattice, AR = 0.7.

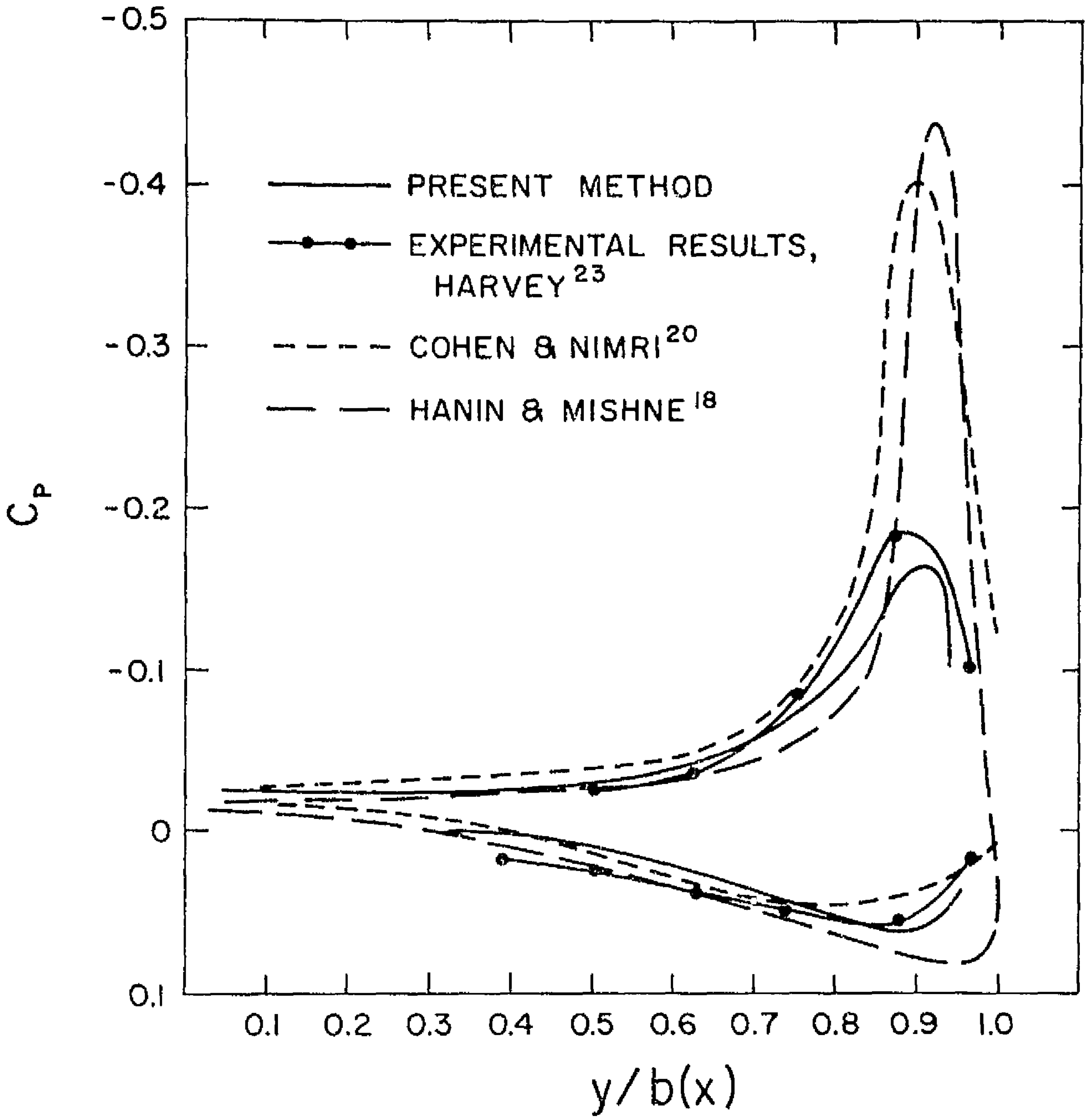

Fig. 6. Upper and lower, spanwise pressure distribution on a steadily rolling delta wing. $\omega_x = -0.2$, $\alpha = 0$, 8 x 8 bound lattice, AR = 0.7, $x/c_r = 0.778$.

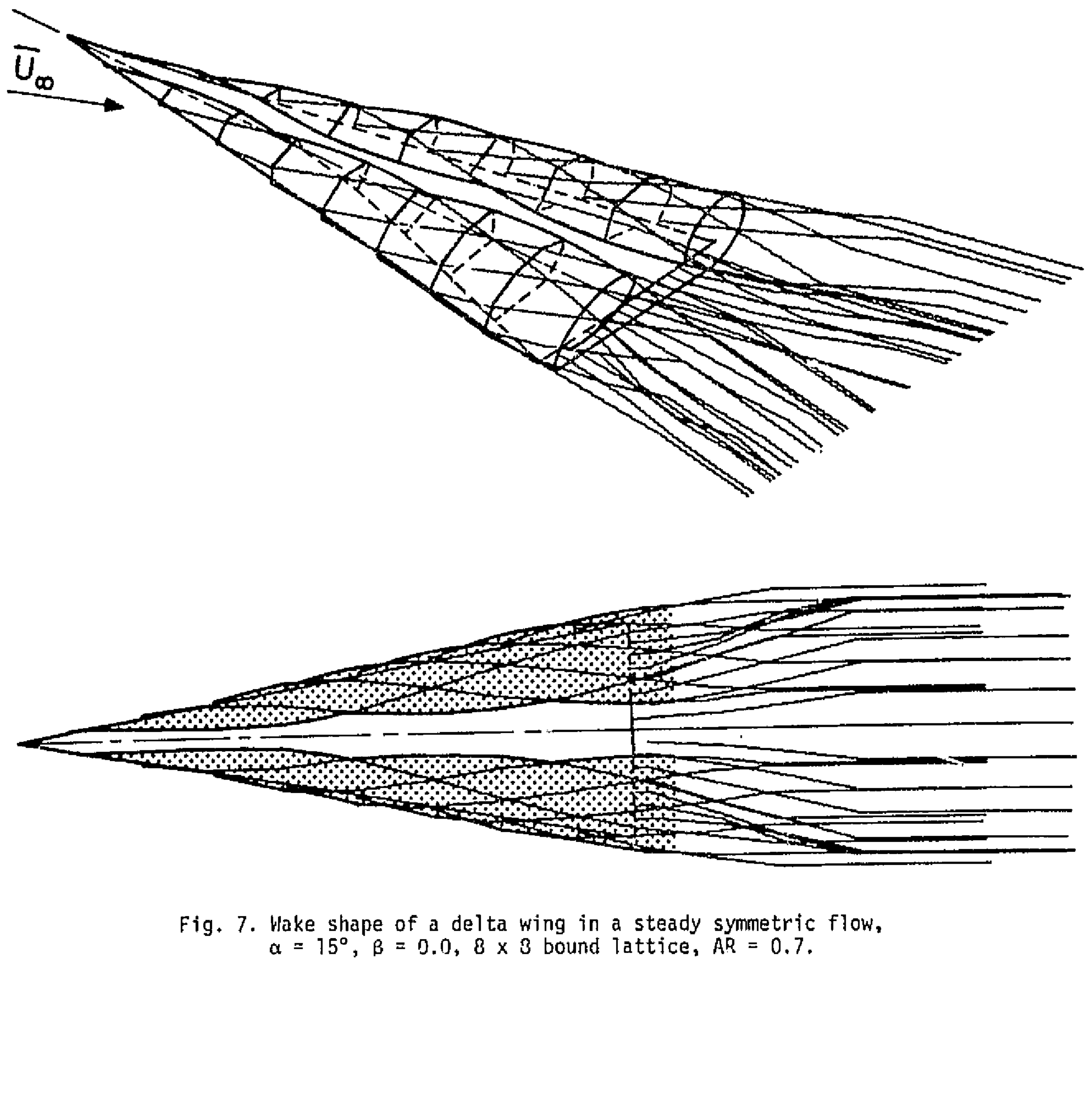

Fig. 7. Wake shape of a delta wing in a steady symmetric flow, α = 15°, β = 0.0, 8 x 8 bound lattice, AR = 0.7.

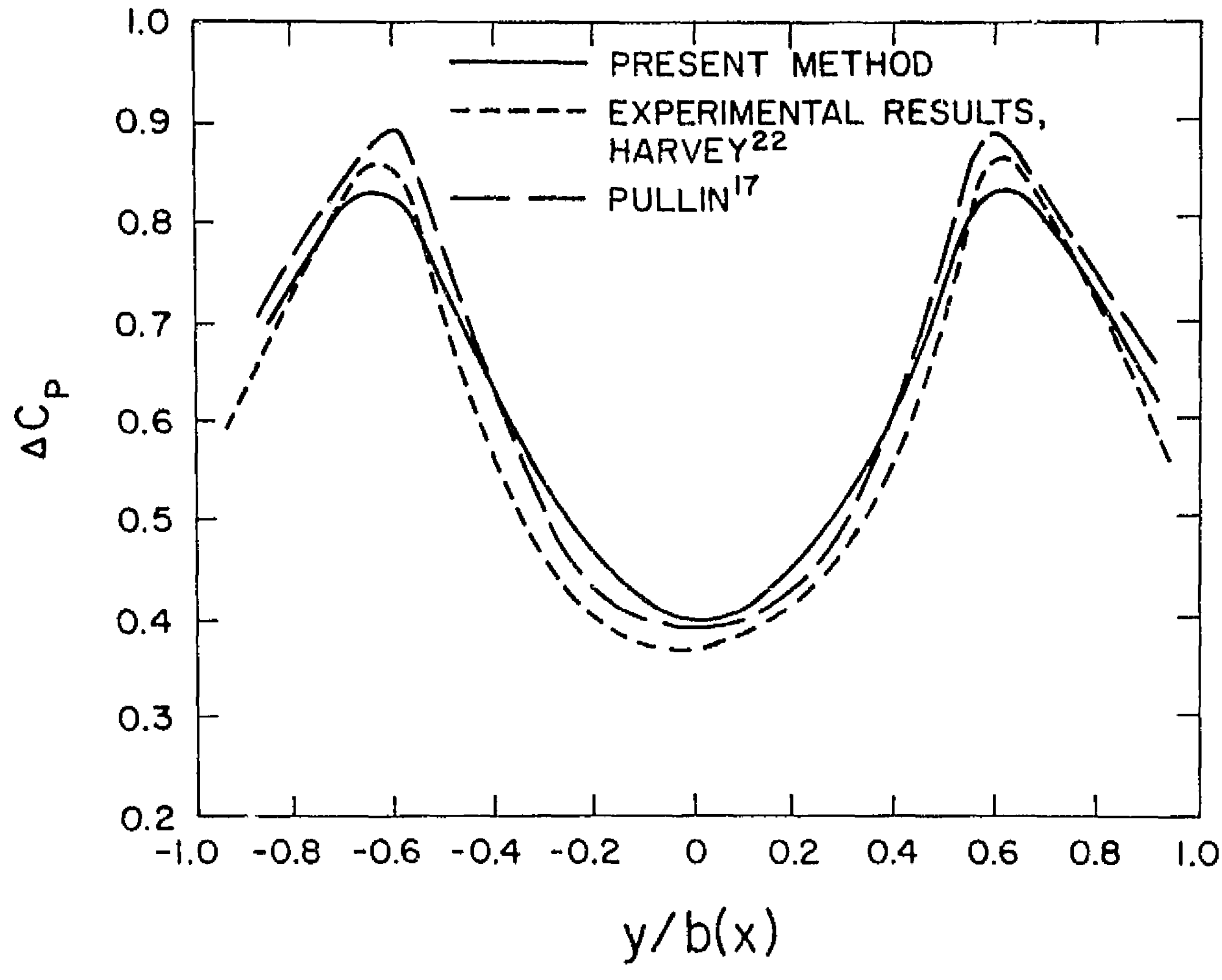

Fig. 8. Net spanwise pressure distribution on a delta wing, $\alpha = 15°$, $\beta = 0$, 8 x 8 bound lattice, AR = 0.7, $x/c_r = 0.395$.

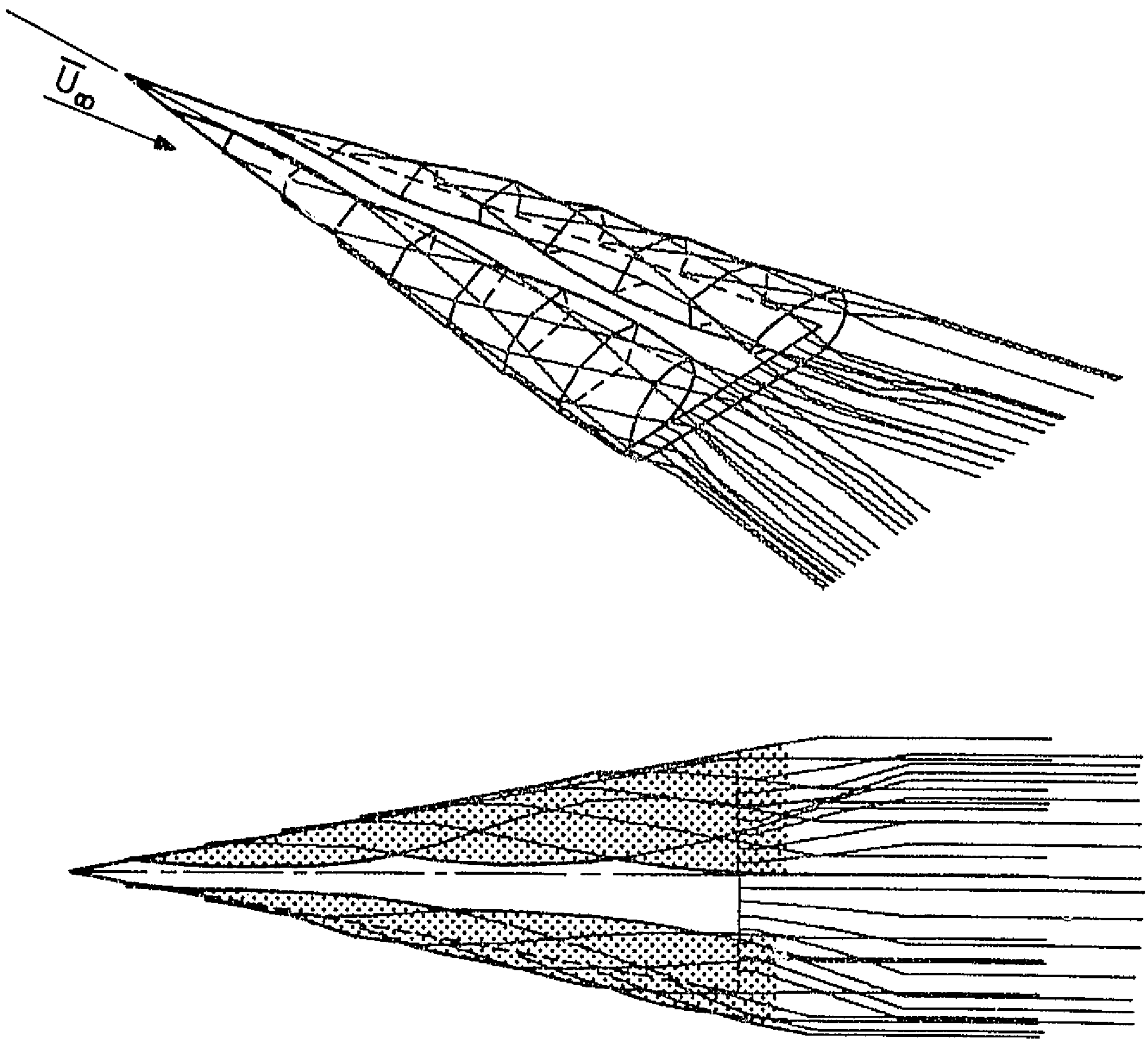

Fig. 9. Wake shape of a yawed delta wing in a steady flow,
α = 15°, β = 5°, 8 x 8 bound lattice, AR = 0.7.

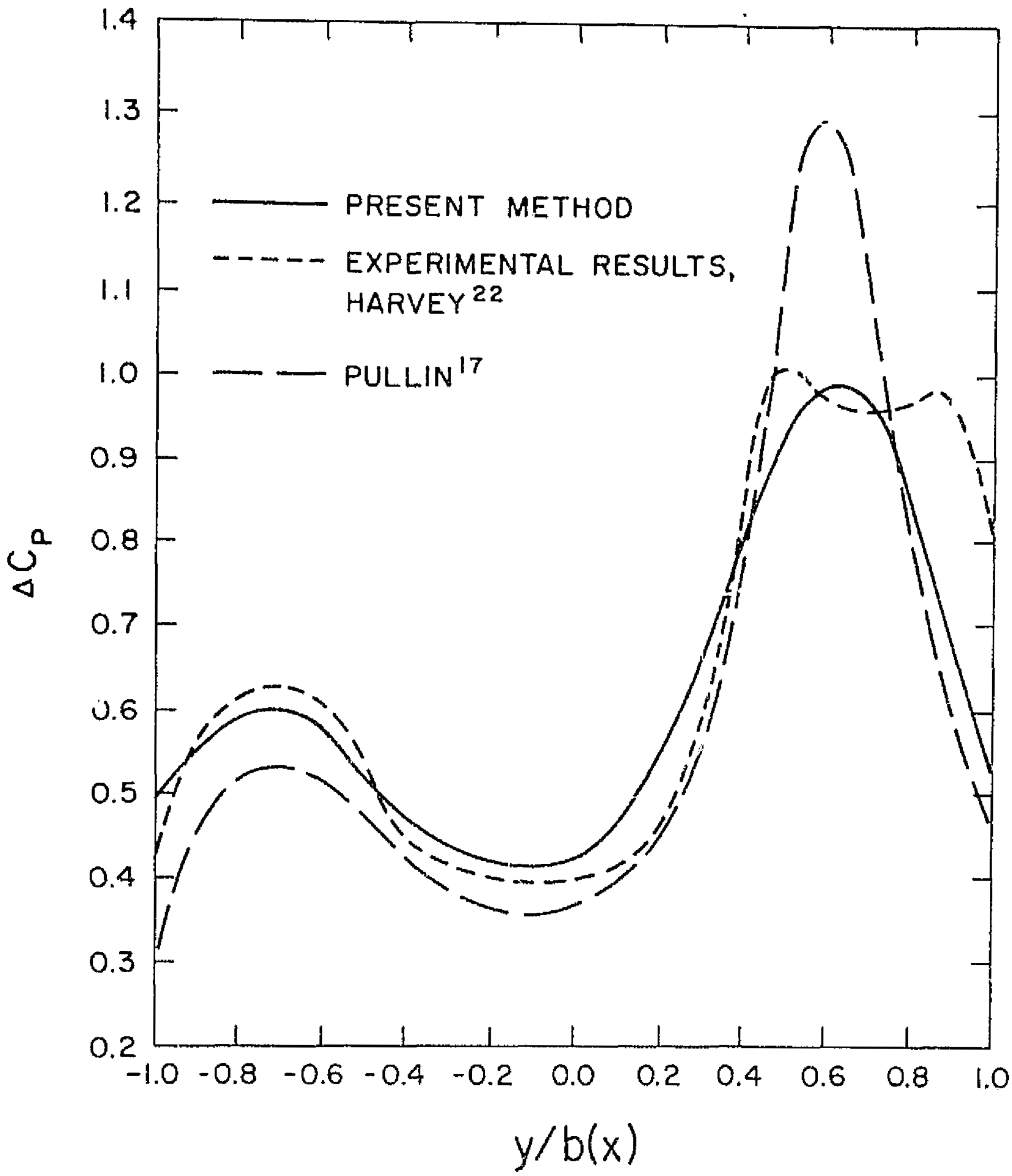

Fig. 10. Net spanwise pressure distribution on a yawed delta wing, $\alpha = 15°$, $\beta = 5°$, 8 x 8 bound lattice, AR = 0.7, $x/c_r = 0.395$.

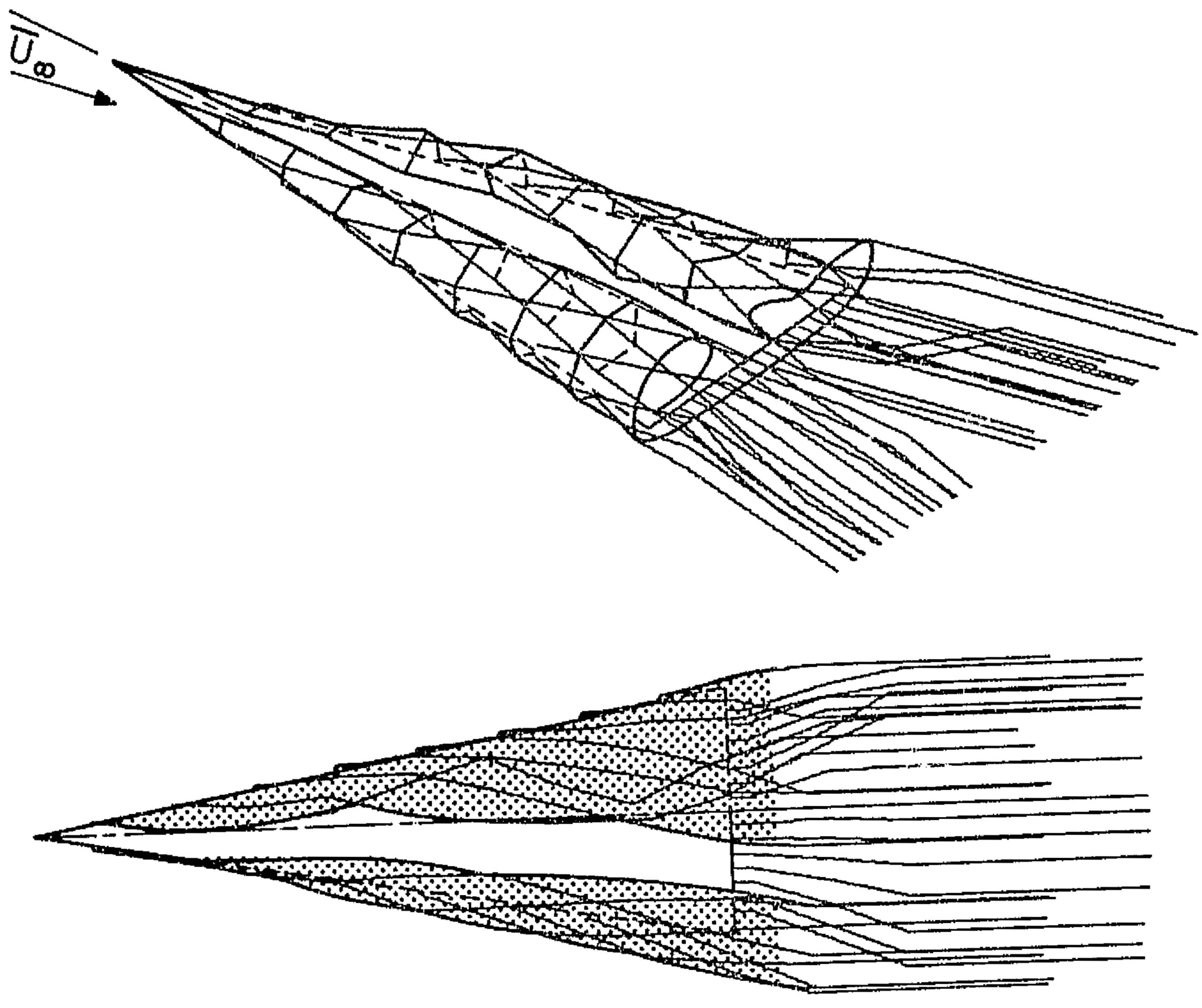

Fig. 11. Wake shape of a yawed delta wing in a steady flow, $\alpha = 15°$, $\beta = 10°$, 8 x 8 bound lattice, AR = 0.7.

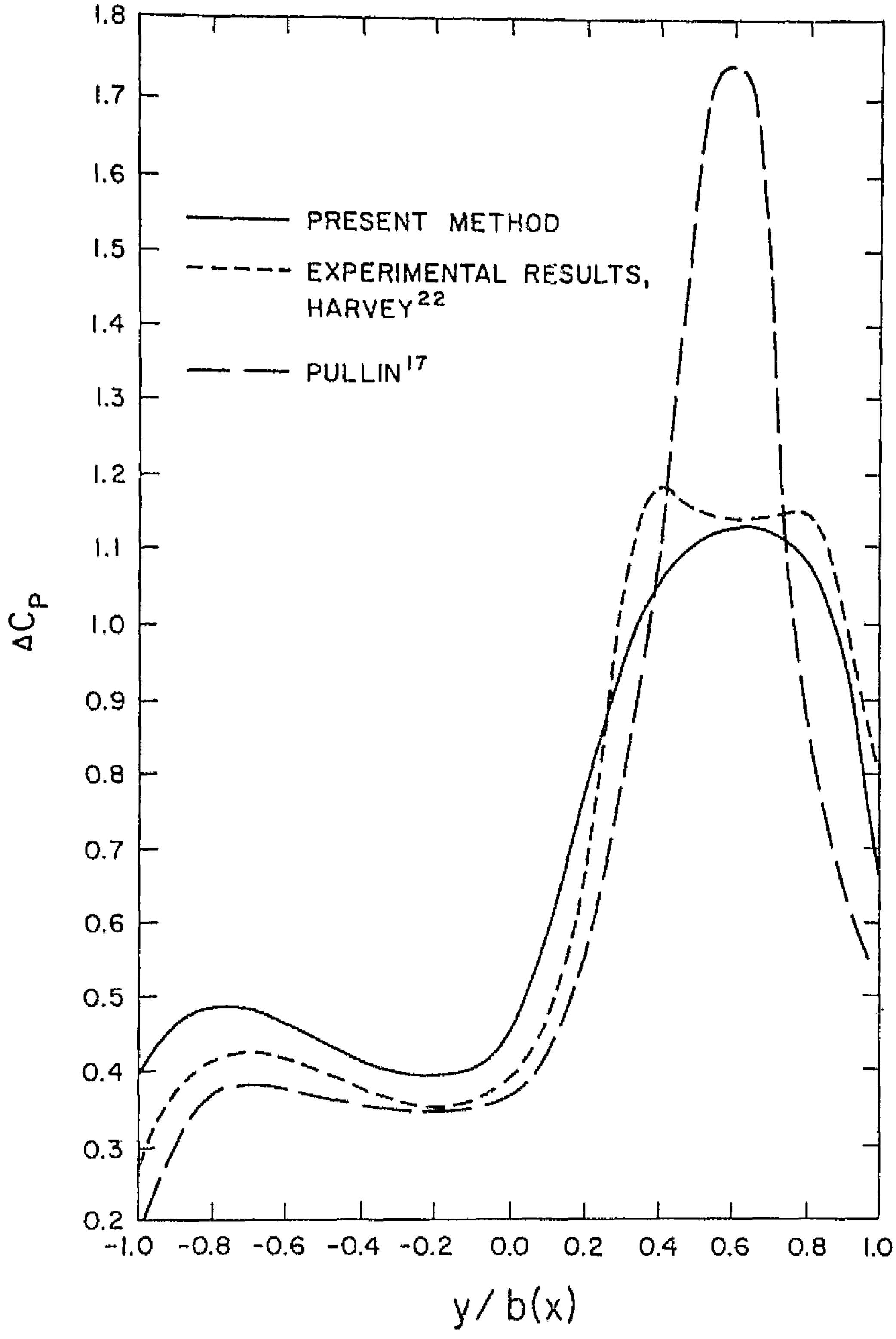

Fig. 12. Net spanwise pressure distribution on a yawed delta wing, α = 15°, β = 10°, 8 x 8 bound lattice, AR = 0.7, x/c_r = 0.395.

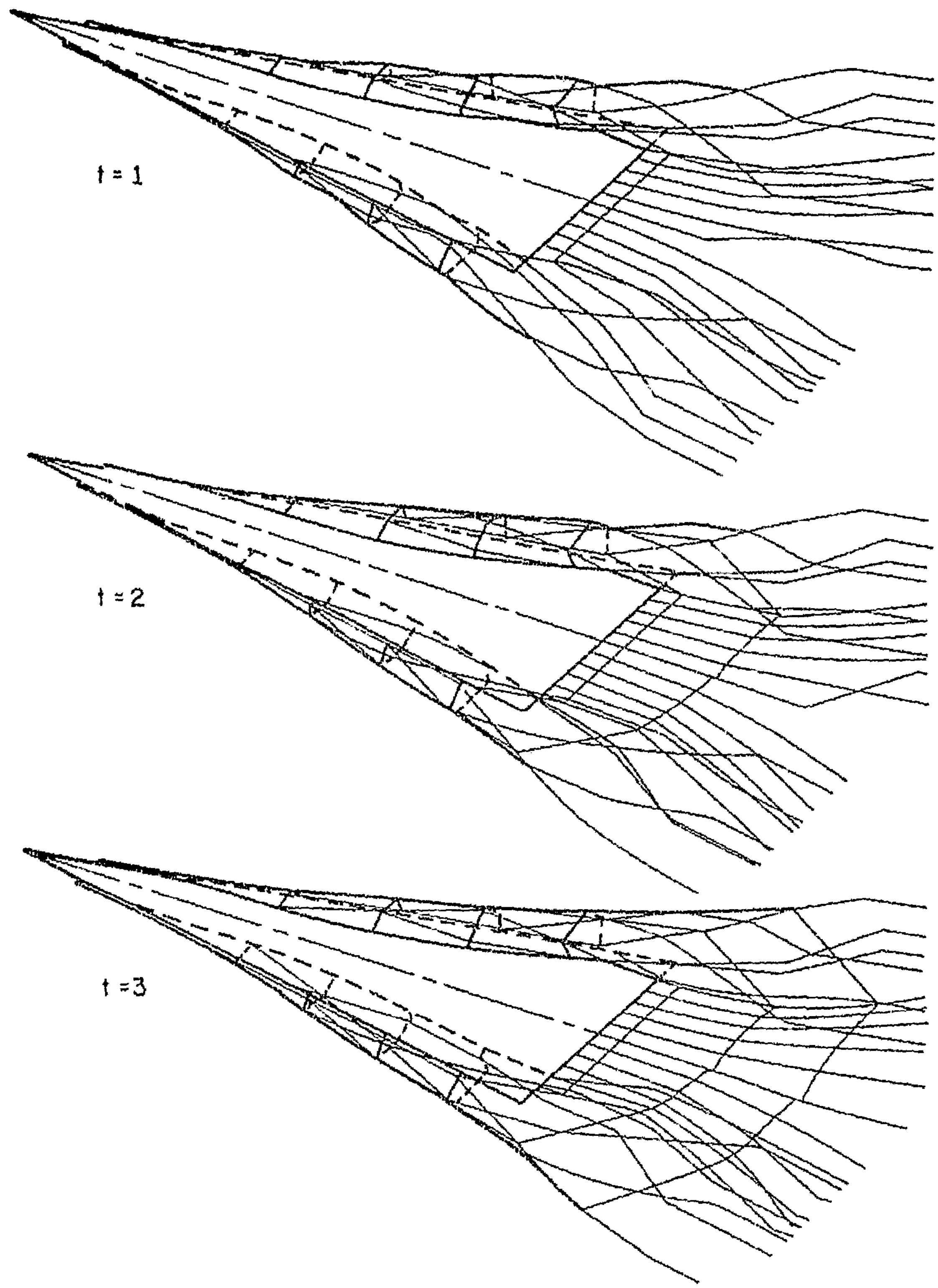

Fig. 13. Wake shape of an unsteadily rolling delta wing, $\omega_x = -0.6 - 0.1 \sin(\pi t/6)$, $\alpha = 0°$, 6 x 6 bound lattice, AR = 0.7.

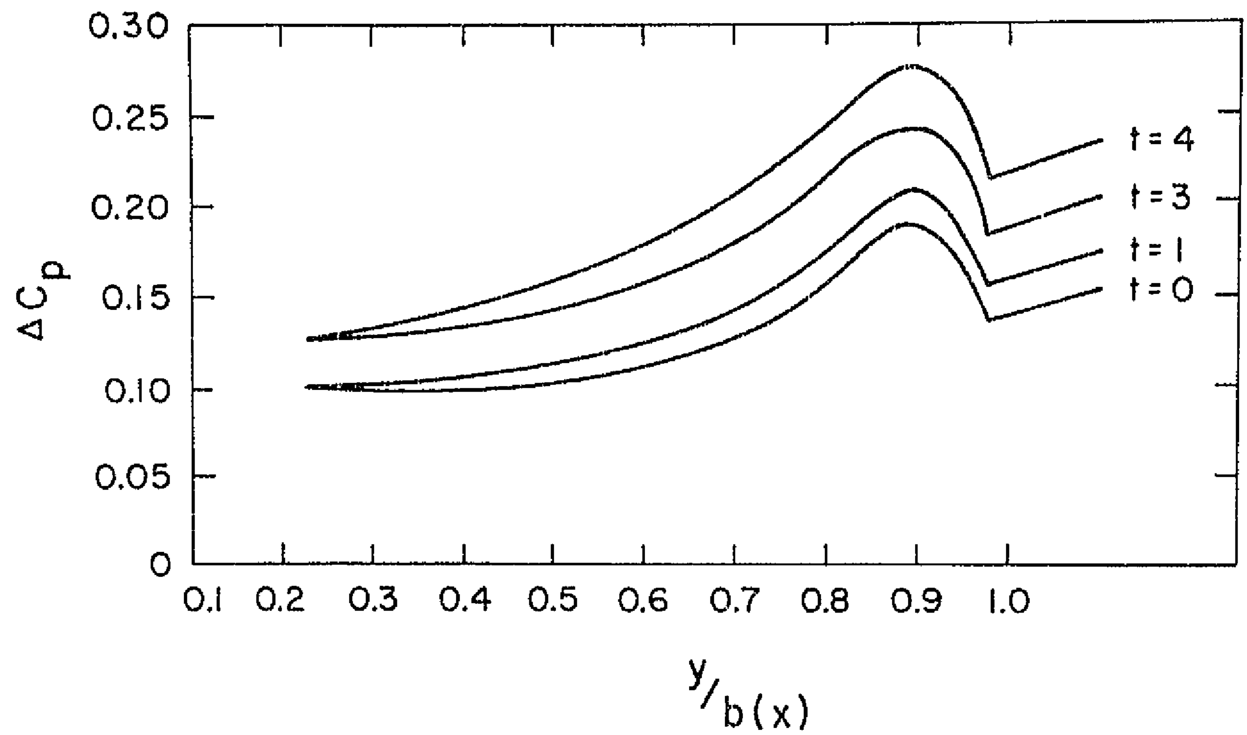

Fig. 14. Variation of the net spanwise pressure distribution with time on an unsteadily rolling delta wing, $\omega_x = -0.4 - 0.1 \sin(\pi t/4)$, $\alpha = 0°$, 6 x 6 bound lattice, AR = 0.7, $x/c_r = 0.65$.

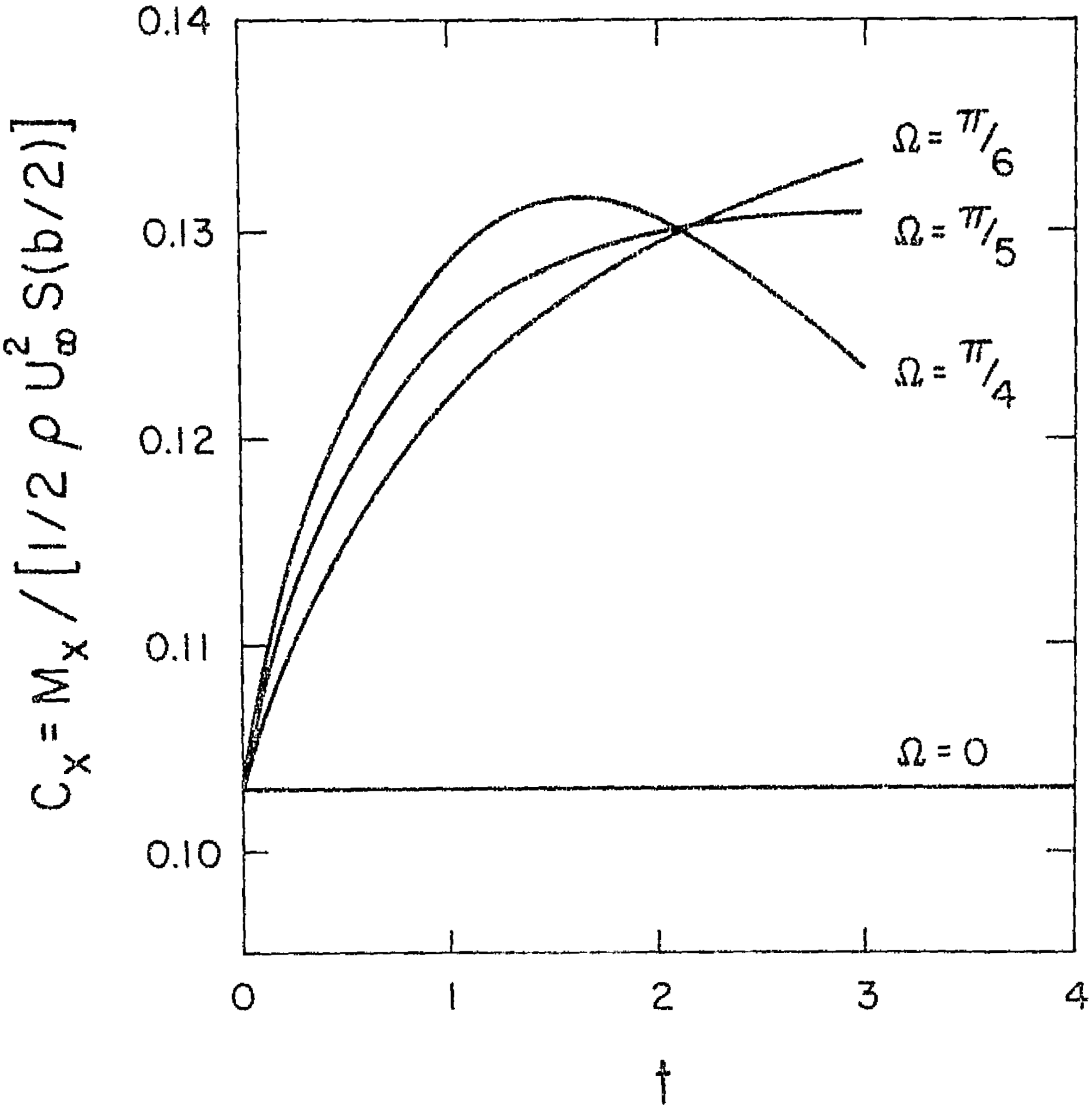

Fig. 15. Variation of the rolling-moment coefficient with the frequency of rolling velocity of an unsteadily rolling delta wing, $\omega_x = -0.4 - 0.1 \sin\Omega t$, $\alpha = 0°$, 6 x 6 bound lattice, AR = 0.7.

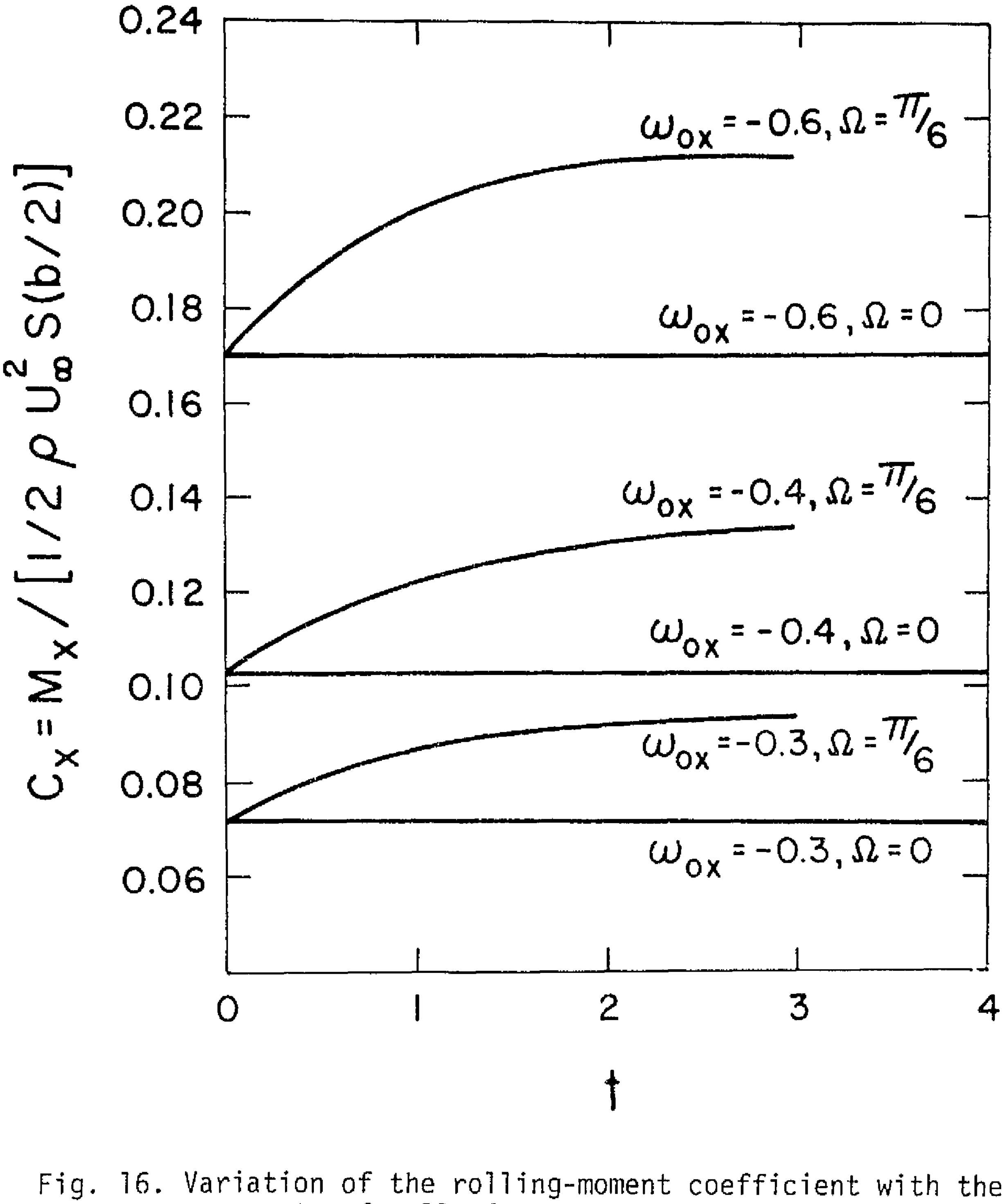

Fig. 16. Variation of the rolling-moment coefficient with the mean rate of roll of an unsteadily rolling delta wing, $\omega_x = \omega_{0_x} - 0.1 \sin\Omega t$, $\alpha = 0°$, 6 x 6 bound lattice, AR = 0.7.

1. Report No.	2. Government Accession No.	3. Recipient's Catalog No.
NASA CR-145235		

4. Title and Subtitle	5. Report Date
THREE DIMENSIONAL STEADY AND UNSTEADY ASYMMETRIC FLOW PAST WINGS OF ARBITRARY PLANFORMS	September 1977
	6. Performing Organization Code
7. Author(s)	8. Performing Organization Report No.
Kandil, O. A.; Atta, E. H.; and Nayfeh, A. H.	
	10. Work Unit No.
	505-15-22-01
9. Performing Organization Name and Address	11. Contract or Grant No.
Virginia Polytechnic Institute and State University Blacksburg, Virginia 24061	NGR 47-004-090
	13. Type of Report and Period Covered
12. Sponsoring Agency Name and Address	Contractor Report
National Aeronautics and Space Administration Washington, D. C. 20546	14. Sponsoring Agency Code

15. Supplementary Notes

Grant Technical Monitor, Dr. E. Carson Yates, Jr.

16. Abstract

The nonlinear discrete-vortex method has been extended to treat the problem of asymmetric flows past a wing with leading-edge separation, including steady and unsteady flows. The problem is formulated in terms of a body-fixed frame of reference and the nonlinear discrete-vortex method is modified accordingly. Although the method is general, only examples of flows past delta wings are presented due to the availability of experimental data as well as approximate theories. Comparison of our results with the experimental results of Harvey for a delta wing undergoing a steady rolling motion at zero angle of attack demonstrates the superiority of the present method over existing approximate theories in obtaining highly accurate loads. Numerical results for yawed wings at large angles of attack are also presented. In all cases, total-load coefficients, pressure distributions and shapes of the free-vortex sheets are shown.

17. Key Words (Suggested by Author(s))	18. Distribution Statement
Unsteady Aerodynamics Nonlinear Aerodynamics Vortex Flow Separation Leading-Edge Flow Separation	Unclassified - Unlimited

19. Security Classif. (of this report)	20. Security Classif. (of this page)	21. No. of Pages	22. Price*
Unclassified	Unclassified	32	$4.00

* For sale by the National Technical Information Service, Springfield, Virginia 22161